sciendo

LATVIAN JOURNAL OF PHYSICS
AND TECHNICAL SCIENCES
2024, N 3

DOI: 10.2478/lpts-2024-0017

FOCUSED POLARIZATION GRATINGS IN AN AZOBENZENE-BASED MOLECULAR GLASSY FILM

A. Ozols*, P. Augustovs, K. Balodis, K. Ozols

Riga Technical University,
Faculty of Materials Science and Applied Chemistry,
3/7 Paula Valdena Str., Riga, LV-1048, LATVIA
*e-mail: andris.ozols@rtu.lv

Holograms recorded by focused light beams have several advantages over usual plane wave holograms such as reduced size, white light readout possibility and others. Focused polarization grating recording in an azobenzene-based molecular glasy film 5,5,5-triphenylpentyl 4-((4-(2-(4-bis(2-hydroxyethyl)amino)phenyl)-1-cyanovinyl)phenyl)dyazenyl)benzoate (which we shortly denoted as B11) is experimentally studied and compared with such grating recording in other materials. It has been determined that focusing manifests itself differently than in other materials, e.g., as in a-As_2S_3 and a-As-S-Se chalcogenide films. Thus, it reduces the holographic grating recording efficiency independently of recording and readout beam polarizations. It has also been found that recording efficiency with circularly and orthogonally *L-R* polarized beams is higher than with linearly polarized *p-p* beams. The highest diffraction eficiency of 26% is achieved with *L-R* polarized unfocused beams.

Recording efficiency grating period dependences for unfocused beams at 200 J/cm^2 exposure and at 1000 J/cm^2 exposure are different with a maxima at 2 μm and 6 μm, respectively. In contrast, recording efficiency grating period dependences for focused beams at 200 J/cm^2 exposure and at 1000 J/cm^2 exposure are the same with the maximum at 6 μm.

The obtained results are discussed in terms of *trans-cis-trans* photoisomerization followed by mass transfer and their light intensity dependence, light electric field gradient force, the photoinduced light scattering and photoelastic forces.

Keywords*: Azobenzene-based molecular glassy films, electric gradient force, holographic polarization gratings, light focusing, recording efficiency, photoelastic force, photoisomerization.*

1. INTRODUCTION

Holograms recorded by focused light beams (focused holograms, image plane holograms) have some properties that make them useful. First, their reduced size is a straightforward way to increase the information density of holographic recording. Holographic versatile discs already have higher capacity than other optical discs (CD, DVD, Blu Ray) [1]. Second, they can be read out with extended broad spectrum light sources, including white light sources [2]. Third, they are used when exposure time is limited and high enough laser light intensities are needed [3]. Fourth, they present a convenient method to convert 3D data to 2D form in computer holography [4].

However, the reduction of hologram size, generally speaking, changes its properties. Among them, diffraction efficiency (DE) and spatial frequency response are of primary importance. The physical processes of focused hologram recording are relatively unexplored. To the authors' knowledge, there are four theoretical papers [5]–[8] devoted to this problem and three experimental ones [3], [9], [10]. In the mentioned experimental papers, only scalar elementary holograms (scalar holographic gratings) have been studied. This paper deals with vector holographic gratings (polarization gratings) when not only recording light intensity but also (and mainly) the spatial distribution of light electric field inside the material is important.

The goal of this paper is to study the properties of holographic grating (HG) recording in an azobenzene film depending on their diameter, grating period, recording beam polarizations and exposure. Previously we have investigated scalar HG recorded with *s-s* polarized beams in amorphous As-S-Se and As_2S_3 chalcogenide films [9], [10]. Here we investigate unfocused and focused polarization HG in azobenzene-based molecular glassy film B11, compare properties between them and with previous results in amorphous chalcogenide films. We conclude that focusing HG in B11 film leads to results different from those in amorphous chalcogenide films, and that polarizations of recording beams do not play a qualitatively important role.

2. EXPERIMENTS AND RESULTS

For our experiments, the sample of the azobenzene-based molecular glassy film was synthesized. The chemical name of the film was 5,5,5-triphenylpentyl4-((4-(2-(4-bis(2-hydroxyethyl)amino)phenyl)-1-cyanovinyl)phenyl)dyazenyl)benzoate which we shortly denoted as B11. Its structural formula is given in Fig. 1. Actually, this name refers to one chromophore molecule of which the film consists. These chromophore molecules are kept together by weak Van der Waals forces.

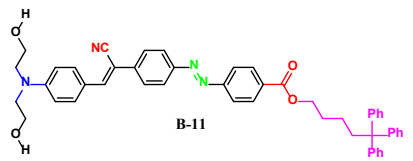

Fig. 1. Structural formula of the studied sample B11. This is an azobenzene molecular glassy film with the thickness d = 1.6 μm put on the glass substrate. Its glass transition temperature is 77 °C. Donor-acceptor push-pull type azochromophore molecule consists of two phenyl rings connected by an azobond –N=N-. Donor is an amino group (blue with N on the left). The main acceptor is carboxylgroup –COO- (right), auxiliary acceptor group is cyano group NC (left).

The absorption spectrum of the sample is presented in Fig. 2.

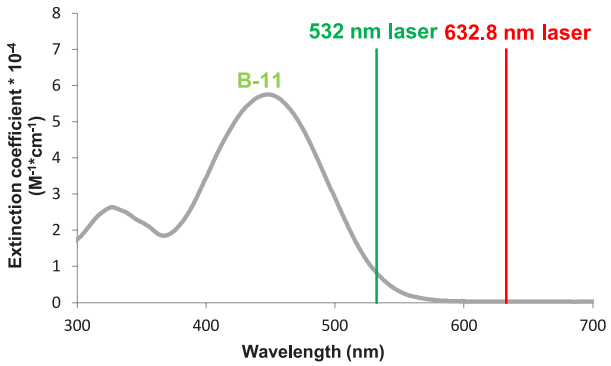

Fig. 2. Absorption spectrum of the B11 film and the laser lines used for holographic grating recording (532 nm) and readout (632.8 nm).

HG recording was carried out by a green Cobolt Samba 60 mW laser at 532 nm but HG readout was performed by a red Melles Griot 35 mW laser at 632.8 nm. HG periods were Λ = 2μm, Λ = 6 μm and Λ = 10.8 μm for unfocused recording beams, and Λ = 2 μm, Λ = 6 μm and Λ = 10 μm for focused recording beams. The $1/e^2$ diameters of all beams were measured by a moving screen method (Fig. 3).

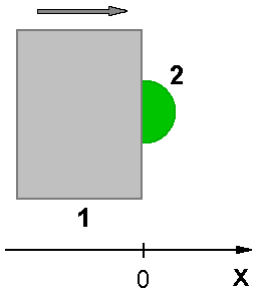

Fig. 3. Moving screen method for laser diameter measurements. 1 – the screen which was gradually moved to the right along the *x*-axis shutting the incident laser beam. 2 – The movement of the screen was started from the position $x = 0$, which corresponded to the half of the transmitted beam power, i.e., to the power ratio $P/P_0 = 0.5$ where P was the transmitted beam power, P_0 was the incident beam power. The ratio P/P_0 as the function of x was measured.

The calculation for the Gaussian light intensity distribution gives the following theoretical expression for this ratio:

$$\frac{P}{P_0} = 0.5[1 - \mathrm{erf}\,(\frac{2\sqrt{2}}{d_0}x)\,, \qquad (1)$$

where d_0 is the $1/e^2$ beam diameter. In our experiments, the power ratio of 0.0142 was technically optimal when small enough beam diameters with the accuracy of 1μm could be measured with our photodetector. Then it follows from Eq. (1) that

$$d_0 = 1.825x. \qquad (2)$$

In the case of unfocused beam HG recording, we measured the recording beam diameter $d_0(1)$ = (1.174 ± 0.007) mm and the readout beam diameter $d_0(2)$ = (1.770 ± 0.021) mm. In the case of focused beam recording when the readout beam was focused as well, we measured $d_0(1)$= (0.139 ± 0.011) mm and $d_0(2)$= (0.104 ± 0.021) mm. Light intensity was defined as $I = P/(\pi d_0^2/4)$, where P is a beam power. This intensity corresponds to the centre of Gaussian laser beam.

The holographic recording and readout setup schematics for unfocused and focused

beam cases are presented in Figs. 4 and 5, respectively. HG recording was carried out by two equal power (P_1=P_2) laser beams whose total intensities $I = (P_1 + P_2)/(\pi d_0^2/4)$ were I = 0.92 W/cm^2 and I= 4.93 W/cm^2, respectively. The recording and readout beam polarization were either linear *p-p-p* or circular *L-R-L*. HG were predominantly scalar in linear polarization case, and predominantly vectorial in circular polarization case. Generally speaking, both types of HG were polarization gratings.

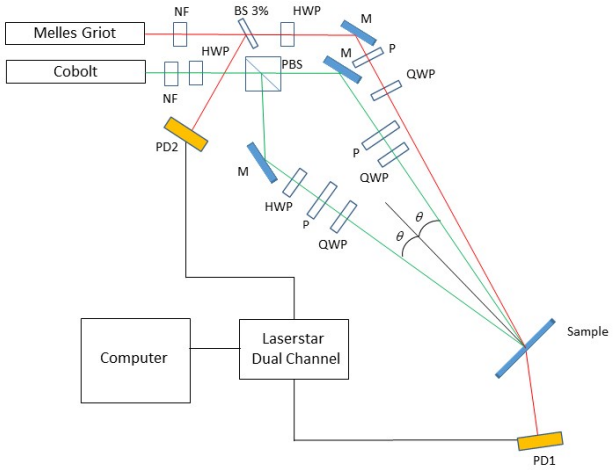

Fig. 4. Holographic recording and readout setup schematic by unfocused laser beams. Notations: NF – neutral density filter, BS 3 % – beam splitter with 3 % reflection coefficient, HWP – half-wave plate, QWP – quarter-wave plate, M – mirror, P – polarizer, PBS – polarization beam splitter, PD1 and PD2 – photodiodes, Laserstar Dual Channel – Ophir Laserstar Dual Channel power meter. Beam formation elements were adjusted for linearly polarized *p-p* beams or circularly polarized *L-R* beams. In the above schematic, the HG recording was performed with *L*- and *R*-polarized beams, readout with *L*-polarized beam.

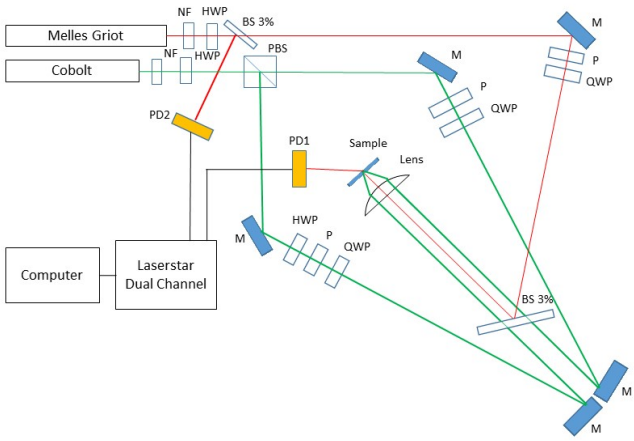

Fig. 5. Holographic recording and readout setup schematic by focused laser beams. Notations: NF – neutral density filter, BS 3 % – beam splitter with 3 % reflection coefficient, HWP – half-wave plate, QWP – quarter-wave plate, M – mirror, PBS – polarization beam splitter, P – polarizer, PD1 and PD2 – photodiodes, Laserstar Dual Channel – Ophir Laserstar Dual Channel power meter. Beam formation elements were adjusted for linearly polarized *p-p* beams or circularly polarized *L-R* beams. In the above schematic, the HG recording was performed with *L*- and *R*-polarized beams, readout with *L*-polarized beam.

Experimental results are presented in Figs. 6–9 and Tables 1–4. The main HG parameter which was measured was diffraction efficiency DE = [P_d/P_i] (%), where P_d was the first-order diffracted beam power and P_i was the readot beam power. DE exposure time dependences for unfocused and focused HG recording at Λ = 6 μm in the case of recording with linearly *p-p* polarized laser beams, and in the case of circularly and orthogonally *L-R* polarized beams are shown in Figs. 6–9. Qualitatively the same DE exposure time dependences were also observed for other HG periods mentioned above. We chose Λ = 6 μm case for the illustration of DE exposure time dependences because the most efficient recording took place at this period.

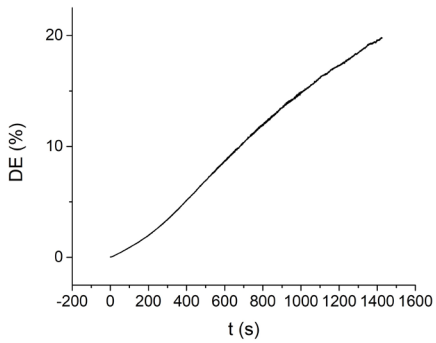

Fig. 6. Diffraction efficiency exposure time dependence for unfocused *p-p* polarized 532 nm laser beams at Λ=6 μm. Readout with *p*-polarized 632.8 nm beam.

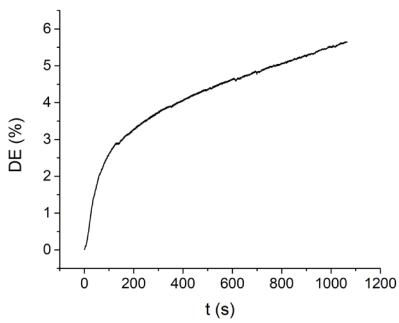

Fig. 7. Diffraction efficiency exposure time dependence for focused *p-p* polarized 532 nm laser beams at Λ=6 μm. Readout with focused *p*-polarized 632.8 nm beam.

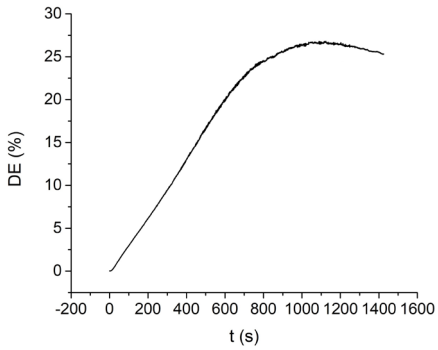

Fig. 8. Diffraction efficiency exposure time dependence for unfocused *L-R* polarized 532 nm laser beams at Λ=6 μm. Readout with *L*-polarized 632.8 nm beam.

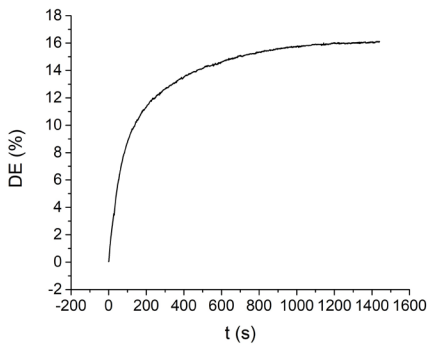

Fig. 9. Diffraction efficiency exposure time dependence for focused *L-R* polarized 532 nm laser beams at Λ=6 μm. Readout with focused *L*-polarized 632.8 nm beam.

Comparison of Figs. 6 and 7 clearly shows that recording with focused laser beams is substantially less efficient, i.e., DE is lower for fixed exposure.

In Figs. 8 and 9, unfocused and focused HG recording DE exposure time dependences are shown in the case of orthogonal circular *L-R* recording beam polarizations.

A comparison of Figs. 8 and 9 shows again that recording with focused laser beams is substantially less efficient also for circularly polarized beams. Thus, focusing reduces the HG recording efficiency independently of beam polarizations. Another conclusion from Figs. 6–9 is that recording with circularly *L-R* polarized beams is

more efficient than with linearly *p-p* polarized beams. The same two conclusions are also valid for other HG periods.

An overview of holographic recording parameters for fixed exposures (*It*) 200 J/cm^2 and 1000J/cm^2 and for all studied HG periods is given in Tables 1–4. To characterise HG recording efficiency more precisely, apart from DE defined above, we also determined specific recording energy, $W=It/\mathrm{DE}$ (J/cm^2) and recording efficiency factor, $\mathrm{REF}=\mathrm{DE}/W$ (cm^2%/J) describing both aspects of DE and material sensitivity. Data in each position of Tables 1–4 correspond to the average values of three measurements to minimise the effect of B11 sample nonuniformity. The maximum relative error does not exceed 10 % for DE and *W*, and 14 % for REF in the case of unfocused beam recording. In the case of focused beam recording, maximum relative errors do not exceed 22 %, 27 % and 35 %, respectively.

As recording and readout beam diameters, $d_0(1)$ and $d_0(2)$, were different, it was necessary to normalize them to equal recording and readout beam parameter case $d_0(1)= d_0(2)$. This was done according to the formula derived in the paper [11]:

$$\mathrm{DE}[d_0(2)=d_0(1))]= (1/3)[1+2d_0(2)^2/d_0(1)^2\,]\,\mathrm{DE}[d_0(2)\neq d_0(1)]\,. \qquad (3)$$

Table 1. HG Parameters in the Case of Unfocused Recording at 200 J/cm^2 Exposure

Beam polarizations	Λ, μm	DE, %	*W*, J/cm^2%	REF, (%cm)^2/J
p-p	2	2.9	68	0.043
L-R	2	7.2	28	0.26
p-p	6	2.6	79	0.033
L-R	6	6.9	29	0.24
p-p	10.8	2.6	77	0.034
L-R	10.8	5.8	35	0.17

Table 2. HG Parameters in the Case of Focused Recording at 200 J/cm^2 Exposure

Beam polarizations	Λ, μm	DE, %	*W*, J/cm^2%	REF, (%cm)^2/J
p-p	2	0.33	620	0.00053
L-R	2	1.5	130	0.012
p-p	6	3.9	50	0.074
L-R	6	4.3	50	0.094
p-p	10	1.7	120	0.015
L-R	10	2.7	80	0.037

Table 3. HG Parameters in the Case of Unfocused Recording at 1000 J/cm^2 Exposure

Beam polarizations	Λ, μm	DE, %	*W*, J/cm^2%	REF, (%cm)^2/J
p-p	2	15	67	0.22
L-R	2	18	55	0.33
p-p	6	16	63	0.25
L-R	6	26	38	0.69
p-p	10.8	16	63	0.25
L-R	10.8	22	45	0.48

Table 4. HG Parameters in the Case of Focused Recording at 1000 J/cm^2 Exposure

Beam polarizations	Λ, μm	DE, %	W, J/cm^2%	REF, (%cm)^2/J
p-p	2	2.4	410	0.0059
L-R	2	4.9	210	0.024
p-p	6	4.5	220	0.021
L-R	6	10	100	0.10
p-p	10	3.2	300	0.011
L-R	10	6.1	170	0.039

The following conclusions can be made by inspecting Tables 1–4.

1. Recording efficiency is higher with unfocused beams than with focused ones. Most easily it can be seen by comparing REF values, which take into account both DE and specific recording energy.
2. Recording efficiency with circularly and orthogonally *L-R* polarized beams is higher than with linearly polarized *p-p* beams. The highest DE=26 % is achieved with *L-R* polarized unfocused beams.
3. Recording efficiency Λ-dependences for *unfocused* beams at 200 J/cm^2 exposure and at 1000 J/cm^2 exposure were *different* with maxima at 2 μm and 6μm, respectively.
4. Recording efficiency Λ-dependences for *focused* beams at 200 J/cm^2 exposure and at 1000 J/cm^2 exposure were *the same* with the maximum at 6μm.

The first two conclusions followed also from Figs. 6–9 in the case of Λ=6 μm. Further we discuss the obtained experimental results.

3. DISCUSSION

Let us consider the first conclusion that unfocused beam HG recording in B11 film is more efficient than unfocused recording. In principle, the recording of HG by spherical waves (as in the case of focused beam recording) is less efficient than by plane waves. It is experimentally proven that maximum DE of HG recorded by spherical waves is smaller by approximately 30 % than maximum DE of HG recorded by plane waves [9]. The main physical reason is the nonuniform spatial frequency response of the recording material. However, in our case the real difference is much higher, and we believe that this is due to the recording efficiency intensity dependence in B11 films. Thus, in a-As_2S_3 films at 632.8 nm we have found that focused beam recording is much more efficient than unfocused recording because of strong light intensity dependence of photostructural changes governing HG inscription [10]. At lesser extent, it is also valid in the case of a-As-S-Se films [9]. Evidently, the light intensity dependence is opposite in B11 films.

HG recording mechanism in B11 film based on literature data [12]–[14] and our observations consisted of four steps.

i. Charge transfer takes place over the aromatic core bridge from donors to acceptors under the influence of 532 nm recording light. As the result, the chromophore molecules which initially were in the *trans* state turn to the *cis* state and reorient perpendicularly to the electric vector of light because of photoinduced quantum transitions.

ii. Further t*rans-cis-trans* photoisomerization cycles takes place according to the spatial polarization modulation of recording light leading to the inscription of volume birefringence grating (VBG).
iii. VBG creates also spatially modulated photoisomerization pressure, which together with electric gradient force results in mass transfer forming surface relief grating (SRG) and/or volume density grating (VDG).
iv. At first, VBG is recorded, and it decays during the readout. The following SRG and VDG grow slower but are stable. There are only SRG and VDG at saturation.

VBG have been recorded much faster than SRG and VDG. Photoinduced birefringence takes place in few seconds whereas relief forms in few hundreds of seconds [14]. Evidently, the lower recording efficiency by focused beams is mainly the result of photoisomerization intensity dependence. As shown by Aleksejeva et al. [14], in the case of B8 films, SRG relief modulation amplitude for intensities higher than 0.4 W/cm^2 decreases, and this decrease is very fast for intensities higher than 1 W/cm^2. The authors explain this phenomenon by too large photosoftening making film unstable. It is highly probable that in B11 films at I=4.93 W/cm^2 photosoftening takes place along with recording, thus decreasing the focused recording efficiency.

The second conclusion about higher recording efficiency with circularly polarized *L-R* beams is more efficient than by linearly polarized *p-p* beams can be explained by the fact that circularly polarized light addresses more chromophores than linearly polarized light already at the stage of VBG [13]. Further, in the case of SRG recording, photoisomerization pressure created by a larger free volume of *cis* form leads to more efficient mass transfer when recorded by *L-R* polarizations compared to *p-p* polarizations [13]. Our atomic force microscope measurements of HG in B11 films have shown that SRG are dominating at large enough exposures reaching relative thickness changes as high as $\Delta d/d$ = 1.0 μm/1.6 μm = 0.625.

The third conclusion about different optimal recording HG periods for unfocused recording at 200 J/cm^2 exposure and at 1000 J/cm^2 exposure (2 μm and 6 μm, respectively) needs more detailed consideration. There are, at least, three factors affecting HG recording efficiency Λ- dependence in azobenzene-based glassy molecular films such as our B11.

First, the most general factor, active in any recording medium, is the spatial resolution of the recording medium, which depends on its atomic structure (size and distribution evenness of photoactive sites), and on the macroscopic inhomogeneities in the bulk and on the surface [15]. Typical spatial resolution of the best silver halide photographic emulsions is expressed by a quantity g= 0.2 μm [15]. This is the minimal image element size, which can be recorded in the emulsion and seen after the emulsion development and is equal to the silver grain size. The resolution of amorphous chalcogenide a-As_2S_3 films is better: $g \leq$ 0.1 μm [15]. The spatial resolution (pixel size) of electronic image capturing devices such as CCD and CMOS is $g >$ 1 μm. The size of azobenzene chromophore molecule (Fig. 1) is about 3 nm [12]. However, the best spatial resolution of azobenzene-based molecular glassy films is about 0.18 μm as shown by our reflection HG recording experiments. This is because photoactive site includes many chromophore molecules taking part in *trans-cis-trans* photoisomerization and mass transfer and because of Rayleigh light scattering by spatial inhomogeneities. Light scattering smears the

interference field inside the medium, and its influence is the highest for small HG periods. In principle, HG recording is possible only if the condition $\Lambda \geq 2g$ holds. Practically, much stronger condition $\Lambda >> g$ must be fulfilled. If the light scattering increases during the HG recording then spatial resolution decreases, and the HG period corresponding to the most efficient recording should increase. This is what one can observe when exposure is increased from 200 J/cm^2 to 1000 J/cm^2 (Tables 1 and 3). We have experimentally observed the increase in light scattering during the exposure. This scattering increase is due to the noise grating recording by scattered light waves and recording waves. Thus, we conjecture that effective grain size is increasing (Fig. 10) shifting the optimum HG period from 2 μm to 6 μm.

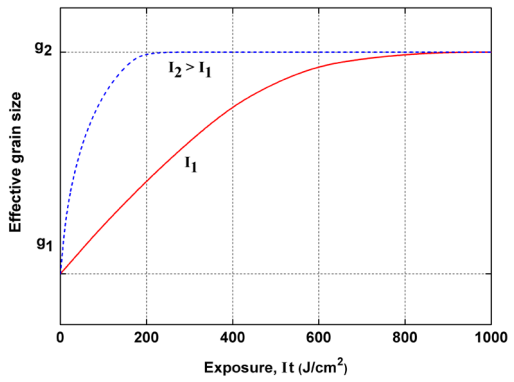

Fig. 10. Effective grain size dependence on exposure and recording light intensity proposed to explain the observed HG recording efficiency Λ- dependences. g_1 is the initial effective grain size and g_2 is the final efective grain size after the 1000 J/cm^2 exposure. Curves correspond to unfocused recording with light intensity I_1 and to focused recording with light intensity I_2 .

Second, the very mechanism of mass transfer due to the light electric field gradient force leads to the certain Λ- dependence. The time-averaged electric gradient force density is [13]:

$$\boldsymbol{f} = \langle (\boldsymbol{P}\nabla)\boldsymbol{E} \rangle , \quad (4)$$

where $\boldsymbol{P}=\chi\boldsymbol{E}$ is the material polarization, χ is the material dielectric susceptibility, $\boldsymbol{E}$ is the light electric field, which harmonically depends on the coordinate along the interference field wave vector (parallel to the sample surface and perpendicular to the bisector between recording beams (see Figs. 4 and 5). Then from Eq. (4) it can be shown both in the cases of *p-p* and *L-R* recording beam polarizations that electric gradient force f is proportional to $1/\Lambda$. Thus, also the surface relief HG recording efficiency is proportional to $1/\Lambda$. This fact explains the recording efficiency decrease at $\Lambda > 2$ μm in the case of unfocused recording at 200 J/cm^2 exposure (Table 1), and at $\Lambda > 6$ μm in the case of unfocused recording at 1000 J/cm^2 exposure (Table 3).

Third, for exposures $It >$ 200 J/cm^2 the deformation of the sample surface becomes significant and the surface elastic forces start to counteract the mass transfer. This corresponds to the necessary increase of surface energy density given by the Gibbs-Helmholtz equation:

$$w_s = \sigma - \partial\sigma/\partial T, \quad (5)$$

where σ is the surface tension, T is absolute temperature [16]. On the other hand, the amplitude of the photoinduced changes of surface tension, $\Delta\sigma$, is directly proportional to sample thickness and inversely proportional to HG period, i.e., $\Delta\sigma \sim d/\Lambda$ [17]. Together with the light scattering this fact facilitates the optimal HG recording period shift from 2 μm to 6 μm when exposure is increased from 200 J/cm^2 to 1000 J/cm^2. The interplay between electric gradient force and elastic force determines the maximal DE values.

The fourth conclusion was that recording efficiency Λ-dependences for focused beams at 200 J/cm^2 exposure and at 1000 J/

cm^2 exposure were the same with the maximum at 6μm. The situation is analogous to the unfocused light beam recording at 1000 J/cm^2 . This can be explained by much higher recording light intensity leading to much higher recording speed. Much more *trans-cis-trans* cycles take place per unit of time with much faster mass transfer and SRG recording. We suppose that already after 200 J/cm^2 exposure the same effective grain size g_2 is reached as in the case of unfocused recording after 1000 J/cm^2 exposure (Fig. 10), and photoinduced scattering shifts the recording efficiency maximum to Λ = 6 μm. This is also stimulated by photoinduced elastic forces, which are inversely proportional to HG period as indicated above.

4. CONCLUSIONS

1. Effect of laser beam focusing on polarization holographic grating (HG) properties is experimentally studied in azobenzene-based molecular glassy 5,5,5-triphenylpentyl 4-((4-(2-(4-bis(2-hydroxyethyl)amino)phenyl)-1-cyanovinyl)phenyl)dyazenyl)benzoate film, which we shortly have denoted as B11 film. This effect in B11 film manifests itself differently than in other materials, e.g., as in a-As_2S_3 and a-As-S-Se chalcogenide films.
2. Focusing reduces the HG recording efficiency independently of recording and readout beam polarizations. The main reason is the recording efficiency intensity dependence of surface relief gratings decreasing at high enough intensities due to the photoinduced softening of the B11 film.
3. Recording efficiency with circularly and orthogonally *L-R* polarized beams is higher than with linearly polarized *p-p* beams. The highest diffraction eficiency of 26 % is achieved with *L-R* polarized unfocused beams. This is due to the fact that circularly polarized light addresses more chromophores than linearly polarized light and that at the stage of surface relief grating recording photoisomerization pressure created by a larger free volume of *cis* form leads to more efficient mass transfer when recorded by *L-R* polarizations compared to *p-p* polarizations.
4. Recording efficiency grating period dependences for unfocused beams at 200 J/cm^2 exposure and at 1000 J/cm^2 exposure are different with maxima at 2 μm and 6 μm, respectively. Recording efficiency is maximal at 200 J/cm^2 because then it is mainly determined by electric gradient force inversely proportional to HG period. At 1000 J/cm^2 the phtoinduced increase of light Rayleigh scattering as well as the photoinduced decrease of photoelastic forces counteracting the HG recording lead to the optimal HG period shift from 2 μm to 6 μm.
5. Recording efficiency grating period dependences for focused beams at 200 J/cm^2 exposure and at 1000 J/cm^2 exposure are the same with the maximum at 6 μm. This difference compared to unfocused beam recording case can be explained by much higher recording light intensity resulting in almost immediate optimal HG period shift from 2 μm to 6 μm due to the photoinduced light scattering and photoelastic forces.

REFERENCES

1. Deepika, G. (2011). Holographic versatile disc. In *2011 National Conference on Innovations in Emerging Technology (pp. 145–146).* Erode, India: IEEE. DOI: 10.1109/NCOIET.2011.5738819.
2. Collier, R.J., Burckhardt, C.B., & Lin, L.H. (1971). *Optical Holography.* New York and London: Academic Press.
3. Kalkum, F., Peithmann, K., & Buse, K. (2009). Dynamics of Holographic Recording with Focused Beams in Iron-Doped Lithium Niobate Crystals. *Optics Express, 17* (3), 1321–1329. DOI: 10.1364/OE.17.001321
4. Hendler, L., & Freedland, S. S.(1986). Image Plane Holography for Holographic Presentation of a Three-Dimensional Data Base. *Comp. & Math. With Appls 12A* (6), 777–784.
5. Schönnagel, G. (1975). Recording and Readout of Volume Holograms in Diffraction-Limited Systems. *Kvant. Elektronika 2* (8), 1622–1628 (in Russian).
6. Siegman, A.E. (1977). Bragg Diffraction of a Gaussian Beam by a Crossed-Gaussian Volume Grating. *J.Opt.Soc.Am 67* (4), 545–550.
7. Moharam, M.G., Gaylord, T.K., & Magnusson, R. (1980). Diffraction Characteristics of Three-Dimensional Crossed-Beam Volume Gratings. *J.Opt. Soc.Am. 70* (4), 437–442.
8. Yakimovich, A.P. (1983). Diffraction Efficiency of Volume Phase Microholograms. *Opt. Spektrosk. 55* (3), 490–494 (in Russian).
9. Ozols, A., Ivanovs, Ģ., & Ļaudobelis, M. (1997). Microhologram Recording in Amorphous Semiconductor Films. *Proc. SPIE 2967,* 276–279.
10. Ozols, A., Saharovs, Dm., & Reinfelde, M. (2006). Holographic Recording in Amorphous As_2S_3 Films at 633 nm. *Journ. of Non-Crystalline Solids 352,* 2652–2656.
11. Ozols, A.O., & Schwartz, K.K. (1982). Photosensitivity Criteria of Media and Optimization of Hologram Recording. *Kvant. Elektronika 9* (12), 2441–2448. (in Russian).
12. Sekkat, Z., & Knoll, W. (2002). *Photoreactive Organic Thin Films.* Orlando, FL: Elsevier Science.
13. Zhao, Y, & Ikeda, T. (2009). *Smart Light-Responsive Materials.* Hoboken, New Jersey: Wiley.
14. Aleksejeva, J., Teteris, J., & Tokmakovs, A. (2013). Azobenzene-Containing Low Molecular Weight Organic Glasses for Optical Recording. *Physics Procedia, 44,* 19–24.
15. Schwartz, K. (1993). *The Physics of Optical Recording.* Berlin: Springer Verlag.
16. Prokhorov, M.A. (ed.) (1992). *Physical Encyclopedia* (vol. 3), *646*. Moscow: Bolshaja Rossiiskaja enciklopedija (in Russian).
17. Jastrzebski, Z.D. (1987). *The Nature and Properties of Engineering Materials.* New York: Wiley.